Revealing the Origin of Typical and Atypical Forms of Atrioventricular Nodal Reentrant Tachycardia with a Compact Computer Model of Rabbit AV Node

Maxim Ryzhii[1], Elena Ryzhii[2]
[1] University of Aizu, Aizu-Wakamatsu, Japan
[2] Fukushima Medical University, Fukushima, Japan

Abstract

In this work, using our recent compact multifunctional model of rabbit AV node, we studied the onset of typical and atypical forms of atrioventricular nodal reentrant tachycardia (AVNRT) and revealed the origin of both forms and their incidence in clinics. We demonstrated for the first time using computer simulations that differences in the effective refractory periods of slow and fast conduction pathways during anterograde and retrograde conduction determine the type (typical or atypical) of AVNRT. The obtained results correspond to the clinical and experimental data and explain the significant prevalence of the typical type over the atypical one.

1. Introduction

Atrioventricular nodal reentrant tachycardia (AVNRT) is the most common type of regular supraventricular arrhythmia. The AVNRT is electrophysiologically classified as typical (slow-fast) and much more rare atypical (fast-slow) forms corresponding to anterograde-retrograde conduction sequence through the dual (fast, FP and slow, SP) pathway structure [1]. The exact nature of the pathways interaction has yet to be established despite numerous attempts to explain the mechanism of AVNRT.

We have recently developed a compact, multi-functional rabbit AV node model based on the simplified two-variable cardiac cell model [2]. The one-dimensional model includes dual pathways, primary pacemaking in the sinoatrial node, and subsidiary pacemaking in slow pathway. Being tuned to the available experimental data [3, 4], the AV node model demonstrates broad functionality, such as filtering high-rate atrial rhythms during atrial fibrillation and atrial flutter with Wenckebach periodicity. In addition, implementing the FP and SP ablation allows each pathway to be considered separately, which is suitable for AVNRT studies. As demonstrated experimentally in mammalian hearts, FP has a significantly longer effective refractory period (ERP) in the case of anterograde conduction (aERP) than SP. This may be a substrate for typical AVNRT at premature stimulation periods shorter than the aERP of FP. On the other hand, the origin of atypical AVNRT is attributed to the retrograde stimulations from ventricles or His bundle (HB).

In this work, along with the typical AVNRT of atrial origin, we simulated scenarios of both typical and atypical AVNRT arising due to HB stimulation. The interaction of electrical conduction between SP and FP was visualized in the form of AV nodal ladder diagrams. The simulations demonstrated that the difference in aERP and retrograde ERP (rERP) between FP and SP determines the prevailing type of AVNRT. Also, the study may explain why atypical AVNRT occurs much less frequently (about 6.4% [5]).

2. Model

The scheme of the compact AV node model is shown in Fig. 1. Each model cell is described by Aliev-Panfilov model [6] given by the following set of ordinary differential equations

$$\dot{V} = c[kV(V-a_1)(1-V) - rV] + I^{coupl} + I^{S1S2}, \quad (1)$$

$$\dot{r} = c[\epsilon_0 + r\mu_1/(V+\mu_2)][-r - kV(V-a_2-1)], \quad (2)$$

where V is the dimensionless transmembrane potential, r is the gate variable, c is the time scaling coefficient, k is the parameter controlling the magnitude of the transmembrane current. Parameters ϵ_0, a_1, a_2, μ_1, and μ_2 determine the conduction characteristics of tissue, $a_1 > 0$ represents the excitation threshold of quiescent excitable cells, while $a_1 < 0$ sets the intrinsic oscillation frequency of the pacemaking cells (gray-shaded in Fig. 1) [7]. The intercellular coupling terms

$$I_i^{coupl} = d_{i-1}(V_{i-1} - \beta_{i-1}V_i) + d_i(-V_i + \beta_i V_{i+1})$$

account for the coupling asymmetry, where d_i are the diffusion coefficients (normalized on dimensionless distance), and the coefficients $\beta < 1$ correspond to the accelerated anterograde and slowed retrograde conduction, and vice versa for $\beta > 1$. I^{S1S2} is the S1S2 premature stimulation current applied to atria and HB (Fig. 1). The parameter values were similar to that in [2] and are based

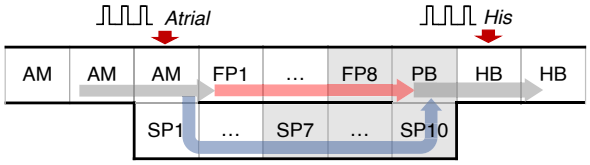

Figure 1. Schematic representation of the rabbit atrioventricular node model. AM - atrial muscle cells, FP - fast pathway cells, SP - slow pathway cells, PB - penetrating bundle cell, HB - His bundle cells. Red vertical arrows denote places of I^{S1S2} application for atrial and HB pacing. The gray-shaded cells indicate AV nodal pacemaker cells.

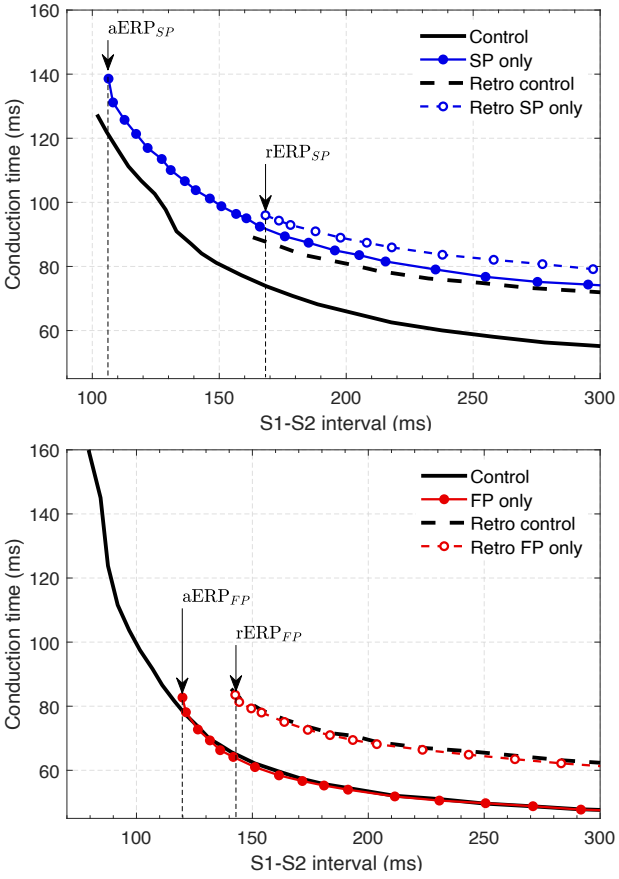

Figure 2. Top panel - experimental conduction curves for control and SP-only (FP ablation) cases with atrial pacing (solid lines) and HB pacing (dashed lines). Bottom panel - experimental conduction curves for control and FP-only (SP ablation) cases with atrial pacing (solid lines) and HB pacing (dashed lines).

on rabbit experimental data [3, 4]. For the sake of simplicity, the sinus node pacemaker part [2] was not included in the present model.

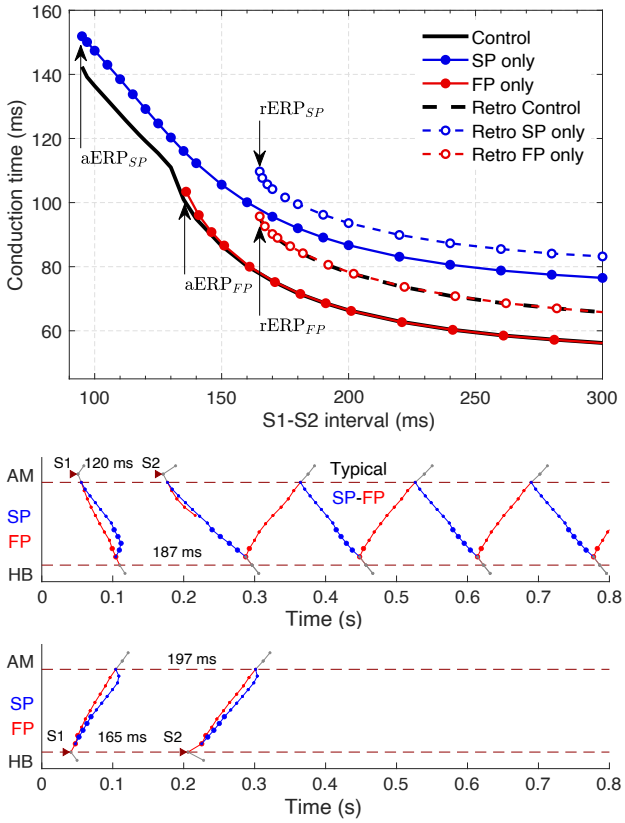

Figure 3. The first model variant with rERP$_{SP} \simeq$ rERP$_{FP}$. Top panel - simulated conduction curves for control and isolated FP and SP conduction in anterograde (solid lines) and retrograde (dashed lines) directions. The middle and bottom panels show ladder diagrams of the AV dual pathway structure with S1S2 atrial pacing (typical slow-fast type AVNRT) and HB pacing (without onset of AVNRT), respectively. Red traces correspond to FP conduction, and blue to SP conduction, with dots denoting model cells. Larger dots mark pacemaker cells. Triangles denote places and moments of S1S2 stimulation.

3. Results and discussion

Experimental conduction curves for rabbit hearts under premature atrial pacing and HB pacing [3] are shown in Fig. 2. The top and bottom panels correspond to the measurements on two groups of rabbits under different ablation (slow and fast) procedures, which explains the dissimilarity in the conduction curve shapes.

The anterograde conduction curves have an exponential-like shape with pronounced bending when conduction changes from FP to SP with a reduced pacing interval. The left part of the conduction curve reflects the conduction via SP at high rates and is characterized by a significant difference between aERP$_{SP}$ and aERP$_{FP}$. This is a fundamen-

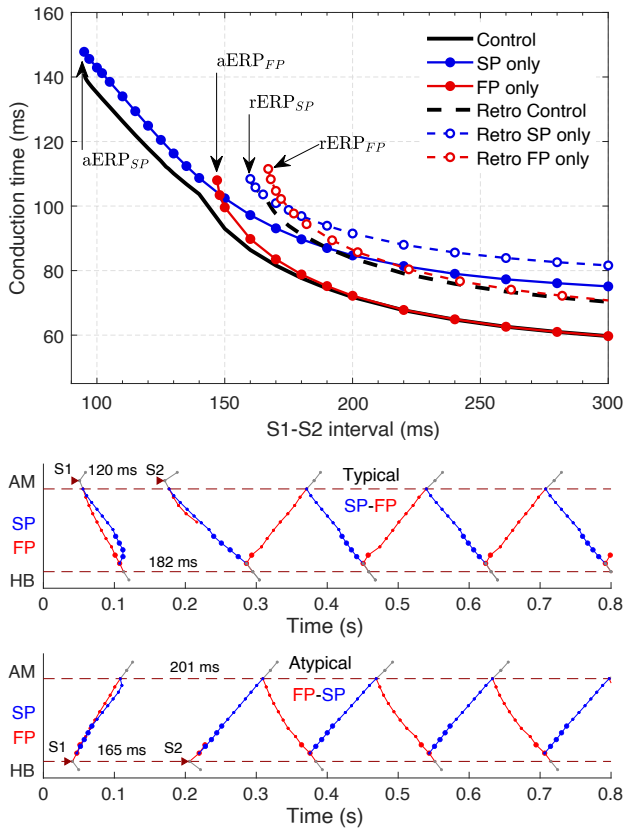

Figure 4. The second model variant with rERP$_{SP}$ < rERP$_{FP}$. Top panel - conduction curves. Middle panel - typical slow-fast AVNRT with atrial pacing. Bottom panel - atypical fast-slow type AVNRT with HB pacing.

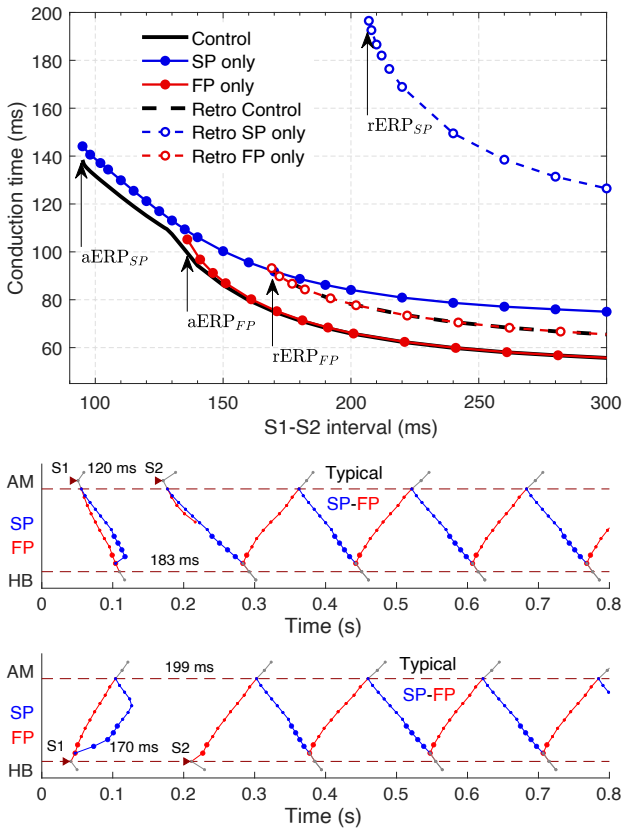

Figure 5. The third model variant with a significant increase of coupling asymmetry in the posterior node extension of SP, reducing its coupling in the retrograde direction (rERP$_{SP}$ ≫ rERP$_{FP}$). In the top panel, the retrograde conduction is slowed in SP with significantly increased rERP$_{SP}$. Anterograde conduction is almost intact. The middle and bottom panels demonstrate typical slow-fast AVNRT with atrial and HB pacing.

tal feature of normal AV node operation under anterograde conduction, allowing effective conduction slowing and fast rhythm filtering, confirmed by experimental and simulation studies [4, 8, 9].

On the other hand, the retrograde conduction curves do not demonstrate a pronounced difference between rERPs in the control and ablation cases (Fig. 2). Moreover, the difference between rERP$_{SP}$ and rERP$_{FP}$ falls within the statistical uncertainty (±10 ms) of the experimental measurements [3]. This allows us to assume that any relation of rERP$_{SP}$ and rERP$_{FP}$ values within the uncertainty period may exist with approximately equal probability. The assumption should not significantly affect the AV nodal operation in general.

We considered AV node model variants with similar anterograde conduction characteristics but different retrograde conduction in SP. The differences were created by altering the SP's coupling asymmetry, particularly in the posterior nodal extension (SP8–SP10 cells in Fig. 1).

In all model variants, atrial pacing (basic S1-S1 interval of 360 ms) with very short S1-S2 intervals (95-126 ms) initiated typical slow-fast type AVNRT (middle panels in Figs. 3–5). Typical AVNRT type is the only possible type in this case due to the condition aERP$_{SP}$ ≪ aERP$_{FP}$. However, both types of AVNRT were observed applying HB stimulation.

The first model variant with original parameters [2] demonstrated very close values of rERP$_{SP}$ and rERP$_{FP}$ (Fig. 3, top panel). Both pathways were in the same state at the moment of HB stimulus application, providing either simultaneous block or retrograde conduction through them. As a result, no AVNRT was observed in the whole range of fast HB pacing S1-S2 intervals (160–175 ms) (Fig. 3, bottom panel). The details of the retrograde conduction in the AV node model can be found in Ref. [2].

The second model variant presents a case with rERP$_{SP}$ < rERP$_{FP}$ obtained with a minor increase of β in the HB cells (Fig. 4). The increase resulted in a range of

Table 1. Characteristics of AVNRT for different model variants with atrial and HB pacing.

Model	aERP$_{SP}$	aERP$_{FP}$	Type (atrial pacing range)	rERP$_{SP}$	rERP$_{FP}$	Type (HB pacing range)
1	95 ms	136 ms	Slow-fast (95–126 ms)	165 ms	165 ms	–
2	95 ms	147 ms	Slow-fast (95–125 ms)	160 ms	167 ms	Fast-slow (160–166 ms)
3	95 ms	136 ms	Slow-fast (95–129 ms)	207 ms	169 ms	Slow-fast (169–206 ms)

S1-S2 intervals (160–166 ms) during HB pacing in which retrograde SP conduction was possible while FP was in a refractory state. Within the range, we observed atypical fast-slow type AVNRT (Fig. 4, bottom panel).

Finally, in the third variant, the coupling asymmetry coefficients β_i in the posterior SP (SP8–SP10 cells) were significantly altered (decreased), reducing the retrograde coupling values and slowing retrograde SP conduction. The alteration neither increased considerably the anterograde SP conduction nor affected the appearance of anterograde AVNRT, but notably shifted up SP retrograde conduction curve and increased rERP$_{SP}$ value well over the rERP$_{FP}$. This led to a wide S1-S2 interval range (169–206 ms) of HB pacing, yielding the typical slow-fast type AVNRT (Fig. 5, bottom panel). As mentioned in [3], the retrograde SP conduction was not observed in some rabbit heart preparations. This situation can be reflected by the SP conduction curve with extremely high conduction times and high values of rERP$_{SP}$, allowing typical AVNRT form only. The observation further increases the probability ratio in favor of the typical slow-fast type of AVNRT (see Table 1). Slow-slow AVNRT observed in humans is beyond the scope of the present work because the model structure is limited to only two functional pathways in the rabbit AV node.

At atrial pacing, due to the significant difference between aERP$_{SP}$ and aERP$_{FP}$ present in a normal intact AV node, only the typical (slow-fast type) AVNRT can be observed. The difference is essential for the normal operation of the AV node during anterograde conduction. In contrast, the retrograde AV nodal conduction is not so critically important for the heart functioning. Our simulations and experiments on rabbit hearts show significant differences in the SP retrograde conduction, including its total absence. This may lead to different rERP$_{SP}$ positions relative to rERP$_{FP}$ on the conduction curve, thus providing both atypical and typical types of AVNRT in the case of HB pacing.

4. Conclusion

Our study demonstrated that the difference in effective refractory period between slow and fast pathways determines the type of AVNRT in both atrial and His bundle pacing. This may explain why the incidence of the typical AVNRT type is much more frequent in clinical observations than the atypical type.

Acknowledgments

The work was supported by JSPS KAKENHI Grant No. 20K12046.

References

[1] D. G. Katritsis and M. E. Josephson, "Classification of electrophysiological types of atrioventricular nodal re-entrant tachycardia: a reappraisal," *Europace*, vol. 15, pp. 1231–1240, 2013.

[2] M. Ryzhii and E. Ryzhii, "A compact multi-functional model of the rabbit atrioventricular node with dual pathways," *Front. Physiol.*, vol. 14, 1126648, 2023.

[3] M. C. Reid, J. Billette, K. Khalife, and R. Tadros, "Role of compact node and posterior extension in direction-dependent changes in atrioventricular nodal function in rabbit," *J. Cardiovasc. Electrophysiol.*, vol. 14, pp. 1342–1350, 2003.

[4] J. Billette and R. Tadros, "An integrated overview of AV node physiology," *Pacing Clin. Electrophysiol.*, vol. 42, no. 7, pp. 805–820, 2019.

[5] D. G. Katritsis, A. Sepahpour, J. E. Marine, G. D. Katritsis, T. Tanawuttiwat, H. Calkins, E. Rowland, and M. E. Josephson, "Atypical atrioventricular nodal reentrant tachycardia: prevalence, electrophysiologic characteristics, and tachycardia circuit," *Europace*, vol. 17, pp. 1099–1106, 2015.

[6] R. R. Aliev and A. V. Panfilov, "A simple two-variable model of cardiac excitation," *Chaos Solitons Fractals*, vol. 7, no. 3, pp. 293–301, 1996.

[7] M. Ryzhii and E. Ryzhii, "Pacemaking function of two simplified cell models," *PLoS ONE*, vol. 17, no. 4, e0257935, 2022.

[8] S. Inada, J. C. Hancox, H. Zhang, and M. R. Boyett, "One-dimensional mathematical model of the atrioventricular node including atrio-nodal, nodal, and nodal-his cells," *Biophys. J.*, vol. 97, pp. 2117–2127, 2009.

[9] A. M. Climent, M. S. Guillem, Y. Zhang, J. Millet, and T. N. Mazgalev, "Functional mathematical model of dual pathway AV nodal conduction," *Am. J. Physiol. Heart. Circ. Physiol.*, vol 300, pp. H1393–H1401, 2011.

Address for correspondence:

Maxim Ryzhii
University of Aizu
Aizu-Wakamatsu 965-8580, Japan
m-ryzhii @ u-aizu.ac.jp